Tunable photonic microwave generation using optically injected semiconductor laser dynamics with optical feedback stabilization

Jun-Ping Zhuang[1] and Sze-Chun Chan[1,2,*]

[1]*Department of Electronic Engineering, City University of Hong Kong, Hong Kong, China*

[2]*State Key Laboratory of Millimeter Waves, City University of Hong Kong, Hong Kong, China*

**Corresponding author: scchan@cityu.edu.hk*

Received December 11, 2012; accepted December 26, 2012;
posted January 3, 2013 (Doc. ID 181525); published January 28, 2013

The period-one (P1) nonlinear dynamics of a semiconductor laser subject to both optical injection and optical feedback are investigated for photonic microwave generation. The optical injection first drives the laser into P1 dynamics so that its intensity oscillates at a microwave frequency. A dual-loop optical feedback then stabilizes the fluctuations of the oscillation frequency. Photonic generation at 45.424 GHz is demonstrated with a linewidth below 50 kHz using a laser with a relaxation resonance frequency of only 7 GHz. The dual-loop feedback effectively narrows the linewidth by over an order of magnitude, reduces the phase noise variance by more than 500 times, and suppresses side peaks in the power spectrum.

OCIS codes: 350.4010, 250.5960, 140.3520.

Photonic microwave generation techniques have attracted considerable attention for transmission of microwave signals over optical fibers with low loss, electromagnetic interference immunity, and wavelength division multiplexing capability [1,2]. The techniques enabled a range of applications, such as radio-over-fiber communication, photonic microwave signal processing, and photonic microwave beamforming, which utilized different photonic components to manipulate microwave signals [1,2]. A number of photonic microwave generation techniques have been extensively investigated. One approach uses mode-locked lasers for monolithic photonic microwave generation, although the frequency tunability is usually restricted by the fixed cavity lengths [3]. Another option is to carefully select two modes in a fiber laser, where frequency tuning is achieved through meticulous mechanical or thermal adjustments [4,5]. Alternatively, an optoelectronic oscillator can generate photonic microwave signals with excellent frequency stability through attaining a high quality factor using a very long fiber loop, where spurious noise at the reciprocal of the round-trip time can be further suppressed using multiple loops [6]. Signal injection into a fiber laser or a semiconductor laser can also increase the microwave modulation depth [7–9]. However, the construction of an optoelectronic oscillator often requires high-frequency components, such as microwave filters, microwave amplifiers, photodetectors (PDs), and optical modulators. The electronic bandwidths of these components limit the frequency tunability of the microwave signals.

Recently, the period-one (P1) nonlinear dynamics of optically injected semiconductor lasers have offered much promise for tunable photonic microwave generation [2]. The approach advantageously allows widely tunable, optically controlled, and single sideband generation of microwave signals [2,10–12]. Although the intrinsic laser noise causes degradation on the frequency stability, improvements have been sought using different methods. Simpson and Doft pioneered a method of locking the P1 dynamics using a stable electronic microwave source, which generated microwave signals up to 17.1 GHz with a linewidth below 1 kHz [13]. Self-injection locking using optoelectronic feedback into the charge carriers of the laser was also demonstrated, but a fast PD and microwave amplifiers were needed [14]. To eliminate the expensive, high-frequency electronic components, dual-beam injection was investigated to generate a 20 GHz signal with a linewidth of 6.2 MHz, which was dependent on the coherence of the two injecting beams [12,15]. Polarization-rotated feedback to the charge carriers is also under much exploration, but strong side peaks separated by the reciprocal of the feedback delay time were reported [16].

In this Letter, photonic microwave generation using the P1 dynamics of a semiconductor laser subject to both optical injection and dual-loop optical feedback is investigated. With the setup in Fig. 1, an optical injection first causes the laser to exhibit P1 intensity oscillation in generating a widely tunable microwave signal. Then, an optical feedback loop is applied to stabilize the fluctuations of the microwave frequency. Additionally, a second feedback loop is introduced to suppress the side peaks caused by the first feedback loop. Overall, the approach requires no high-frequency feedback electronics. The microwave frequency is also widely tunable, as no microwave filters are used. The P1 oscillation frequency is much more stable than that generated using optical

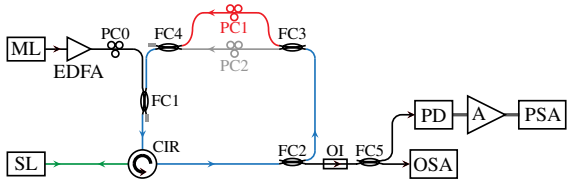

Fig. 1. (Color online) Schematic of a semiconductor laser under optical injection and dual-loop optical feedback. ML, master laser; SL, slave laser; PC, polarization controller; FC, fiber coupler; CIR, circulator; OI, optical isolator; OSA, optical spectrum analyzer; PD, photodetector; A, microwave amplifier; and PSA, power spectrum analyzer.

injection alone, where the microwave linewidth is reduced by at least an order of magnitude and the phase noise variance is reduced by more than 500 times because of the dual-loop optical feedback.

Figure 1 shows the setup using single-mode semiconductor lasers in a master-slave configuration. The slave laser (SL) is a distributed-feedback laser (Nortel LC111-18) packaged with a fiber pigtail. It is biased at 2.4 times its 25 mA threshold and temperature-stabilized at 20°C. When free-running, the laser emits 1.7 mW in the fiber pigtail at optical frequency $\nu_0 = 193.72$ THz and has a relaxation resonance frequency f_r of 7 GHz. The master laser (ML; HP 8168A) emits continuous-wave light that is subsequently amplified by an erbium-doped fiber amplifier (EDFA), split by a 90∶10 fiber coupler FC1, delivered through a circulator, and injected into the SL. The optical injection power in the fiber pigtail is denoted as P_i, while the optical frequency detuning of the injection from ν_0 is denoted as f_i. The injection parameters (P_i, f_i) can be varied by adjusting the ML and the EDFA. The polarization of the injection light is optimized to match that of the SL by adjusting a polarization controller PC0. The emission from the SL passes through the circulator into a 60∶40 coupler FC2, an optical isolator, and split by a 50∶50 coupler FC5 for detection by an optical spectrum analyzer (HP 86140B) and a PD (Newport AD-10ir), which has a 43 GHz electrical bandwidth. The PD output is connected to a 26.5 GHz microwave amplifier (Agilent 83006A) and monitored by a power spectrum analyzer (PSA; Agilent N9010A). All fibers are fixed on the setup to minimize mechanical fluctuations.

Optical feedback into the SL is first prohibited by disconnecting polarization controllers PC1 and PC2 from the rest of the setup. With proper optical injection, the SL exhibits P1 dynamics so that it simultaneously emits two optical frequency components separated by a P1 oscillation frequency f_0, as the optical spectra in Figs. 2(a)–2(c) show. With $(P_i, f_i) = (4.5$ mW, 17.3 GHz), (7.2 mW, 40.9 GHz), and (7.6 mW, 98.4 GHz) in Figs. 2(a)–2(c), the generated P1 frequency is $f_0 = 24$, 45, and 100 GHz, respectively. In each spectrum, the frequency component labeled by the red arrow is the regeneration of the injection at $\nu_0 + f_i$, where the dashed line marks the free-running optical frequency ν_0 for reference. The other component at $\nu_0 + f_i - f_0$ is generated by the P1 dynamics and can be attributed to the laser cavity resonance with a red-shifting caused by the injection [17]. At the PD, beating of the two components generates the output microwave signal at f_0. The two optical frequency components have equal amplitudes so that the output microwave power is maximized for any fixed input optical power to the PD. Figure 2(d) shows the injection parameters required for generating such equal-amplitude P1 dynamics when f_0 is continuously tuned up to 100 GHz.

To examine the quality of the output microwave signal, the power spectrum monitored by PSA is shown in Figs. 3(a)–3(c). The injection is set at $(P_i, f_i) = (4.5$ mW, 17.3 GHz) so that $f_0 = 24$ GHz. Noises of the lasers lead to fluctuations of f_0 and so a relatively broad 3 dB microwave linewidth of 8.2 MHz is observed in Fig. 3(a). In order to stabilize the fluctuations, a single-loop optical feedback is introduced by connecting PC1 as in Fig. 1 but keeping PC2 disconnected. The emission from the SL is sent through the 40%-port of FC2, a 50∶50 coupler FC3, the red path with PC1, another 50∶50 coupler FC4, and looped back to FC1 that directs 10% power to the circulator for feeding back into the SL. The unused ports of FC1 and FC4 are terminated to avoid back-reflections. The polarization of the feedback light is adjusted by PC1 to match that of the SL. The resultant power spectrum is shown in Fig. 3(b). The central peak of the power spectrum is clearly narrowed by such single-loop optical feedback. The microwave linewidth is significantly reduced to below 50 kHz, as limited by the resolution of PSA. However, the single-loop feedback also gives strong side peaks separated from the central peak by multiples of 8.0 MHz, which equals the reciprocal of the delay time for light propagation in the feedback loop. The feedback loop comprises the red, the blue, and twice the green paths in Fig. 1. Then, for suppressing the side peaks, a second feedback loop is included by finally connecting PC2, as Fig. 1 shows. The second loop comprises the gray, the blue, and twice the green paths. The feedback light polarization is adjusted to match that of the SL by PC2. The reciprocal of the light propagation delay time of the second loop is 8.4 MHz, which is different from that of

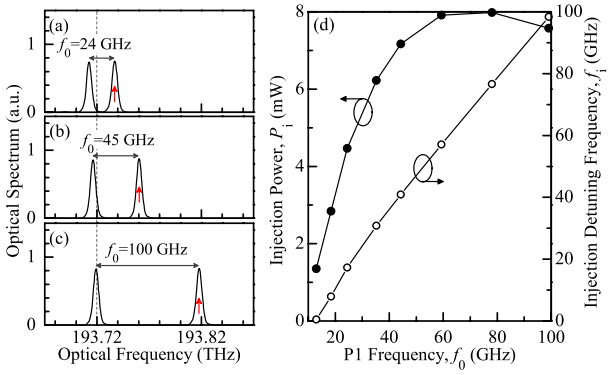

Fig. 2. (Color online) (a)–(c) Optical spectra of the SL emissions in P1 dynamics subject to optical injection with $(P_i, f_i) = (4.5$ mW, 17.3 GHz), (7.2 mW, 40.9 GHz), and (7.6 mW, 98.4 GHz), respectively. Resolution bandwidth, 7.5 GHz. (d) (P_i, f_i) required for equal-amplitude P1 dynamics at different f_0.

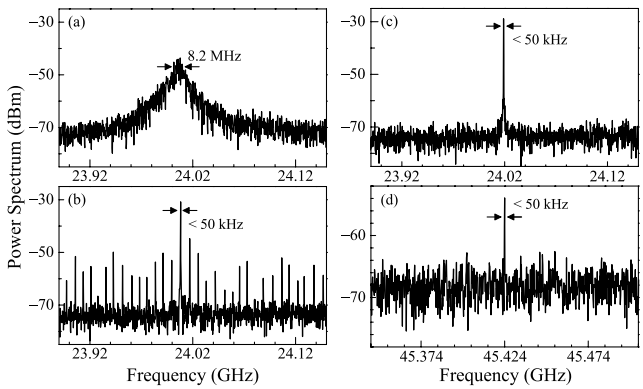

Fig. 3. Power spectra of the SL emissions (a) without feedback, (b) with single-loop feedback, (c) with dual-loop feedback when $(P_i, f_i) = (4.5$ mW, 17.3 GHz), and (d) with dual-loop feedback when $(P_i, f_i) = (7.2$ mW, 41.3 GHz).

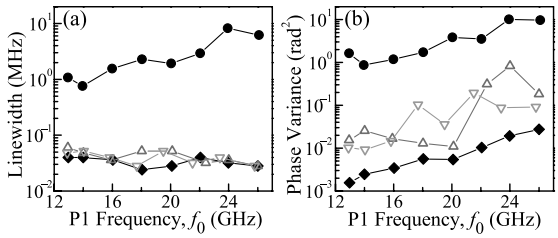

Fig. 4. (a) Linewidth and (b) phase noise variance as functions of f_0. Circles, no feedback; triangles, single-loop feedback; diamonds, dual-loop feedback.

the first loop. As a result of the combined effect of the two loops, a clean spectrum is obtained in Fig. 3(c). The dual-loop optical feedback clearly suppresses the side peaks around the central peak, while the central peak continues to have a narrow linewidth below 50 kHz. To demonstrate dual-loop feedback stabilization at millimeter wave frequencies, f_0 is tuned to 45.424 GHz by setting $(P_i, f_i) = (7.2\ \text{mW}, 41.3\ \text{GHz})$ in Fig. 3(d). The spectrum is recorded by immediately connecting the output of the PD to a millimeter wave spectrum analyzer (Agilent E4448A), where the microwave amplifier in Fig. 1 is bypassed due to its limited bandwidth. Nonetheless, a narrow peak at $f_0 = 45.424$ GHz is still observed with a linewidth below 50 kHz.

The stabilization of the frequency fluctuations of the P1 dynamics is more thoroughly illustrated in Fig. 4, as f_0 is continuously tuned. The SL is subject to no feedback (circles), single-loop feedback with only PC1 connected (up-triangles), single-loop feedback with only PC2 connected (down-triangles), and dual-loop feedback with both PC1 and PC2 connected (diamonds), while f_0 is tuned by adjusting the injection parameters, according to Fig. 2(d). In Fig. 4(a), the linewidth of the central peak of the power spectrum is plotted. The linewidth is reduced by at least an order of magnitude when either a single-loop or the dual-loop feedback is applied. The frequency purity at f_0 is further quantified by the associated phase noise variance in Fig. 4(b). The phase variance is estimated by integrating the single sideband power spectrum normalized to the central peak and offset by 3–100 MHz [13,18]. According to Fig. 4(b), the dual-loop feedback significantly reduces the phase variance by more than 500 times, while single-loop feedbacks are less effective in reducing the phase variance due to the presence of side peaks.

In summary, a semiconductor laser in P1 dynamics under both optical injection and dual-loop optical feedback is investigated for photonic microwave generation. The optical injection can be adjusted to tune the generated microwave frequency f_0 over a wide range beyond f_r, while the dual-loop feedback stabilizes the frequency fluctuations and suppresses the associated side peaks. Using the laser with $f_r = 7$ GHz, generation at $f_0 = 45.424$ GHz is demonstrated with a linewidth below 50 kHz. The approach applies the P1 dynamics for tunable and stable photonic microwave generation without high-frequency feedback electronics.

The work described in this Letter was fully supported by a grant from the Research Grants Council of Hong Kong, China (Project No. CityU 111210).

References

1. J. P. Yao, J. Lightwave Technol. **27**, 314 (2009).
2. X. Q. Qi and J. M. Liu, IEEE J. Sel. Top. Quantum Electron. **17**, 1198 (2011).
3. C. Y. Lin, F. Grillot, N. A. Naderi, Y. Li, and L. F. Lester, Appl. Phys. Lett. **96**, 051118 (2010).
4. G. Chen, D. Huang, X. Zhang, and H. Cao, Opt. Lett. **33**, 554 (2008).
5. Y. N. Tan, L. Jin, L. Cheng, Z. Quan, M. Li, and B. O. Guan, Opt. Express **20**, 6961 (2012).
6. X. S. Yao and L. Maleki, IEEE J. Quantum Electron. **36**, 79 (2000).
7. S. L. Pan, Z. Z. Tang, D. Zhu, D. Ben, and J. P. Yao, Opt. Lett. **36**, 4722 (2011).
8. S. L. Pan and J. P. Yao, Opt. Lett. **35**, 1911 (2010).
9. B. Romeira, K. Seunarine, C. N. Ironside, A. E. Kelly, and J. M. L. Figueiredo, IEEE Photon. Technol. Lett. **23**, 1148 (2011).
10. I. Gatare, M. Sciamanna, M. Nizette, H. Thienpont, and K. Panajotov, Phys. Rev. E **80**, 026218 (2009).
11. M. Pochet, N. A. Naderi, Y. Li, V. Kovanis, and L. F. Lester, IEEE Photon. Technol. Lett. **22**, 763 (2010).
12. A. Quirce and A. Valle, Opt. Express **20**, 13390 (2012).
13. T. B. Simpson and F. Doft, IEEE Photon. Technol. Lett. **11**, 1476 (1999).
14. S. C. Chan and J. M. Liu, IEEE J. Sel. Top. Quantum Electron. **10**, 1025 (2004).
15. Y. S. Juan and F. Y. Lin, IEEE Photon. J. **3**, 644 (2011).
16. T. B. Simpson, J. M. Liu, M. AlMulla, N. Usechak, and V. Kovanis, IEEE J. Sel. Top. Quantum Electron. **19** (2013).
17. S. C. Chan, IEEE J. Quantum Electron. **46**, 421 (2010).
18. S. C. Chan and J. M. Liu, IEEE J. Quantum Electron. **41**, 1142 (2005).